University of Bahrain

Department of Physics

PHYCS426: Advanced Computational Physics

Spring 2022

From the Ising model to Nano-granular systems

Instructor

Dr. Jawad Mohamed Taher Mohamed Alsaei

Authors

Asif Bin Ayub	20191251
Kumail Abdulaziz Radhi	20196080

Contents

1 Introduction

As children, we are fascinated by magnets. Magnets seem like the most mysterious objects. With time, most people tend to lose interest in understanding how magnets work – but not us. Continuing the pursuit of understanding magnets, in this project we try and explain various forms of magnetisms and associated properties using the Ising model.

About a hundred years ago, Wilhelm Lenz introduced a model for magnetic properties in solids. Ernst Ising*, who was a student of Lenz solved the model in 1D. He concluded that there can't be phase transitions, unlike in real magnets. Thinking that the same is true in higher dimensions, the model was dismissed. But in 1944, Lars Onsager solved the Ising model in 2D, and demonstrated the existence of phase transitions. And thus began a new chapter in our understanding of magnets.

In this project, we use the Ising model to simulate a ferromagnetic material and study various properties such as magnetization, susceptibility and the specific heat. We confirm the existence of a phase transition into paramagnetism and characterize the associated Curie temperature T_C. We then study the effects of system size and exchange energy on the properties of the system.

We also simulate antiferromagnetism with Ising model and investigate the various properties. The identify the Néel temperature that corresponds to phase transition into paramagnetism. Lastly, we introduce general spin direction to the 2D Ising model, and see how it changes the properties.

It is fascinating that Ising model manages to capture aspects of real magnets despite its simplicity. In fact, Ising model captures the phase transition behaviour of many other phenomena. This hints at what is known as "universality" [1] – how the same behaviour shows up in seemingly unrelated phenomena.

Let's hope that you're still interested in learning about magnets after all this!

* After whom the Ising model is named

2 Theory

2.1 Types of magnetic materials [2]

When one thinks about a magnet, it usually refers to a ferromagnet. In the classical picture, a magnet is composed of two opposing magnetic poles, creating what is called a "dipole"*. The strength of a magnet is characterized by its **dipole moment** ($\boldsymbol{\mu}$). The basic expression of diploe moment is given by: $\boldsymbol{\mu} = I\boldsymbol{A}$

Here, I is the current flowing in a looped circuit, with $\boldsymbol{A}$ representing the vector area enclosed by the loop. This suggests that the source of magnetism requires the existence of current loops of some sort (classically).

The dipole

(a) (b)

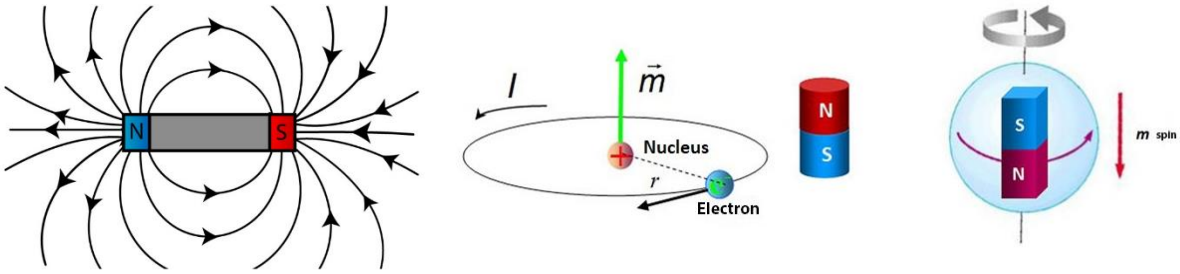

Figure 2.1: (a) Illustration of a typical bar magnet (Source: skyrocket.co.uk)
(b) Magnetic moment associated with electronic orbit in an atom (Source: imamagnets.com)

These currents originate at the atomic level resulting from electron's orbit around the nucleus.

The electrons in the atomic shells are determining the magnetic properties of the material. If the atom has unpaired electrons that atom exhibit paramagnetic properties. In our report we will deal with atom having unpaired electron(s) as a spin†.

In this report we are studying 3 types of magnetic materials: Ferromagnetic, paramagnetic, and antiferromagnetic material.

- **Paramagnet:** It is composed of atoms or ions that have permanent atomic dipole, as mentioned above have unpaired electrons. These dipoles don't have any tendency to be aligned together. Exerting external magnetic field align them resulting a transient magnetization. The net magnetization of paramagnet is zero in the absence of external magnetic field.

* Famously, magnetic monopoles don't exist (as far as we know)
† In Ising model (introduced later) we're deal with spins not atoms.

- **Ferromagnet:** The opposite of paramagnets, ferromagnets have a permanent magnetization even in the absence of magnetic field. They are strongly aligned with presence of external magnetic field; this refers to the very large positive susceptibility. But ferromagnets are not ferromagnets forever, in the higher temperatures after a critical temperature called Curie temperature the ferromagnet becomes paramagnet. That's due to destroying the ordering of spins.

- **Antiferromagnet:** In contrast with ferromagnets, the spins in antiferromagnets tend to be antiparallel to each other cancelling their magnetization. That's because the unpaired electrons have opposite directions that their intrinsic magnetic moments cancel each other. Similar to ferromagnetic, there is critical temperature after it happens an antiferro-para phase transition. It is called Néel temperature.

2.2 Magnetic properties studied [2]

Magnetic susceptibility χ indicates the extent of magnetization in response to an external magnetic field. Magnetic materials can be classified according to their susceptibilities. The sign of it indicates whether a substance is attracted or repelled. Studying susceptibility as a function of temperature give as informative results about the nature of magnetism and properties of magnetic materials. As shown in figure*, it is studied to find the Curie and Néel temperature for ferro- and antiferro-materials, respectively.

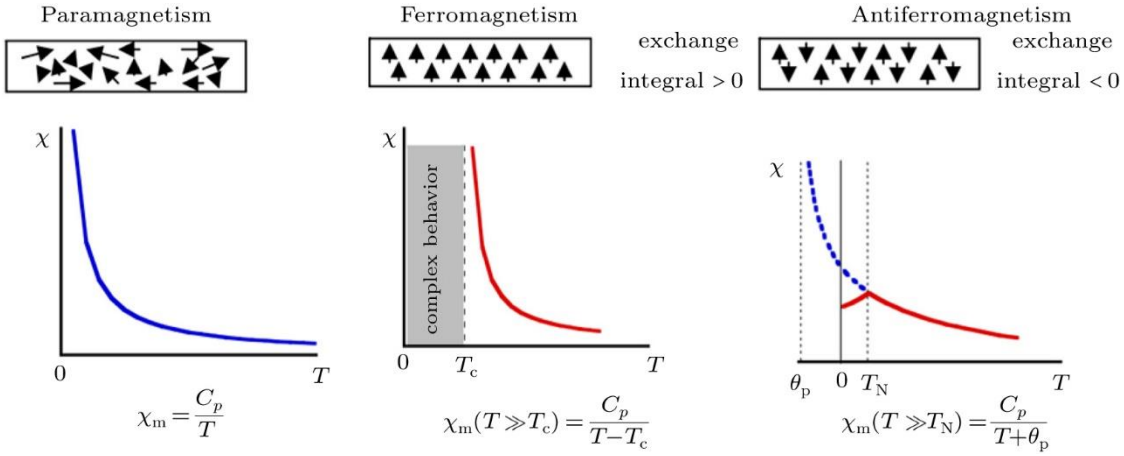

Figure 2.2: Susceptibility with temperature for para-, ferro- and antiferro-materials. (Source: cpb.iphy.ac.cn)

Coercive field B_C is the strength of applied magnetic field required to demagnetize a ferromagnetic material. For a permanent magnet, we need a larger coercive field to demagnetize it, in other words we need a larger energy. Coercivity depends on how fast we change the magnetic field. Coercive field depends on temperature, as the temperature of the system increase the coercive field decreases. This is explained that the material loses its ferromagnetic nature and goes gradually through phase transition to paramagnetic phase, where paramagnets have zero coercive field i.e. no energy required to demagnetize it.

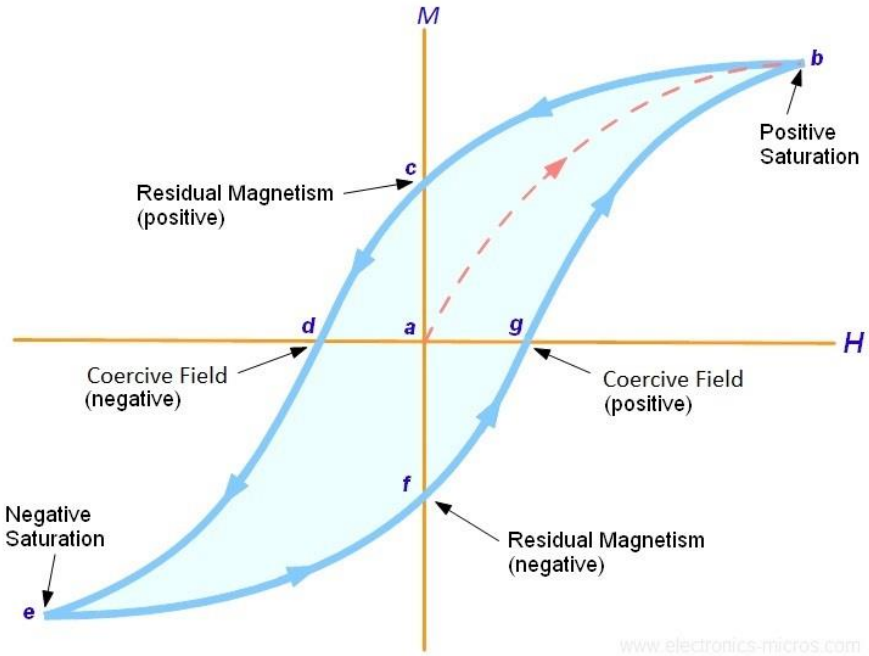

Figure 1.3: The hysteresis loop of ferromagnets. (Source: electronics-micros.com)

2.3 The Ising Model [5]

The Ising model is a toy model of magnetism that simplifies the picture of magnetism at the atomic level. It models the interactions of atoms by treating them as small magnets "spins" that is either up or down. There are two competing "forces"* at play:

1) The interaction of magnetic moments† of atoms with each other and external magnetic field.
2) The tendency of external temperature to induce random fluctuations in the system.

* Not actually forces, it's called like this to simplify the idea.
† Called "spins" in Ising model.

The Hamiltonian for the Ising model contains two terms: Exchange term and Zeeman term $\mathcal{H}_{total} = \mathcal{H}_{spins} + \mathcal{H}_{Zeeman}$. Where the spins including the interaction between nearest neighbours (nn) only. That is:

$$\mathcal{H}_{total} = -\sum_{<i,j>} J_{ij} S_i S_j - \mu B S_i$$

The model is simulated by using Monte Carlo Metropolis method, which depends on the randomness of flipping spins and checking if the energy of the system is increases or not. And this process goes over all spins over the grid in what is called a Monte Carlo step*. The figure below shows the flowchart of Monte Carlo Metropolis method.

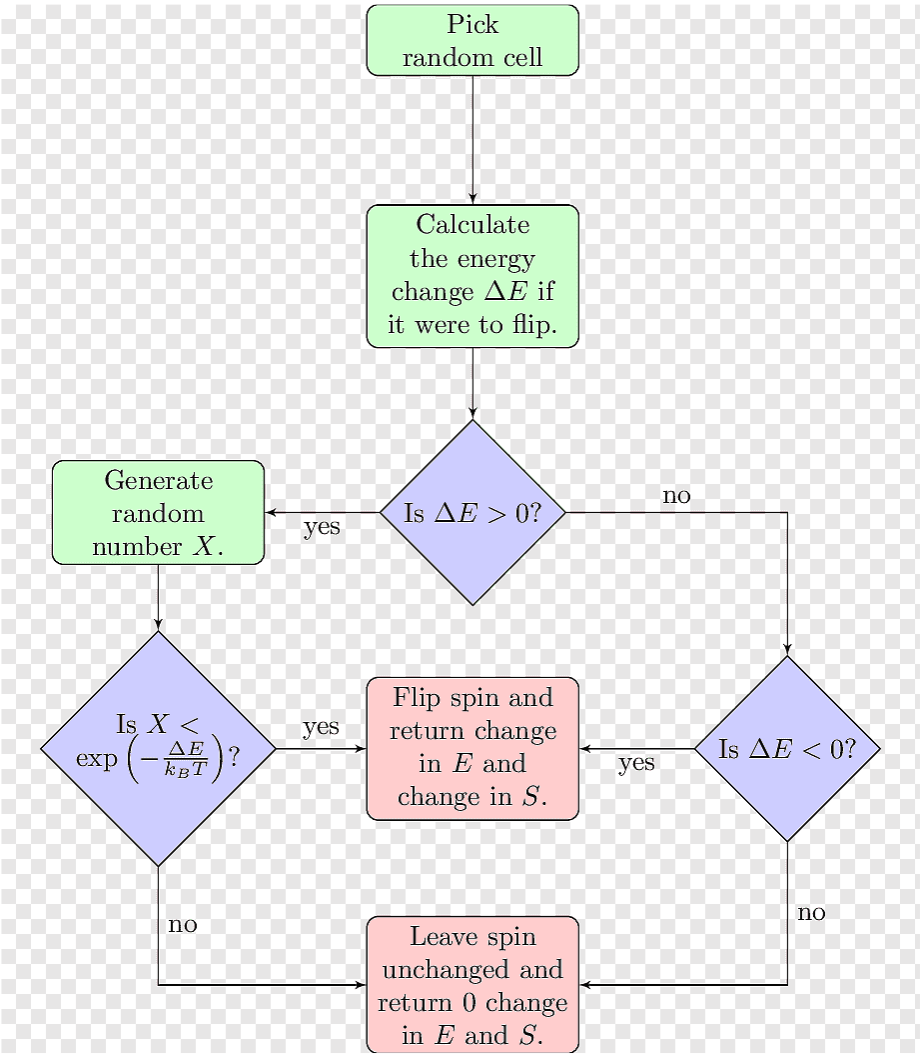

Figure 2.4: The flowchart of the Metropolis algorithm. (Source: pngwing.com)

* Abbreviated as MC steps from now on

3 The Classic Ising Model in 2D & 3D

3.1 Existence of ferro-para phase transition

To demonstrate the ferro-para transition, we first consider the Ising model *in the absence of external magnetic field*. Plotting the average magnetization* $\langle M \rangle$ with increasing temperature, we obtain the plots similar to the following:

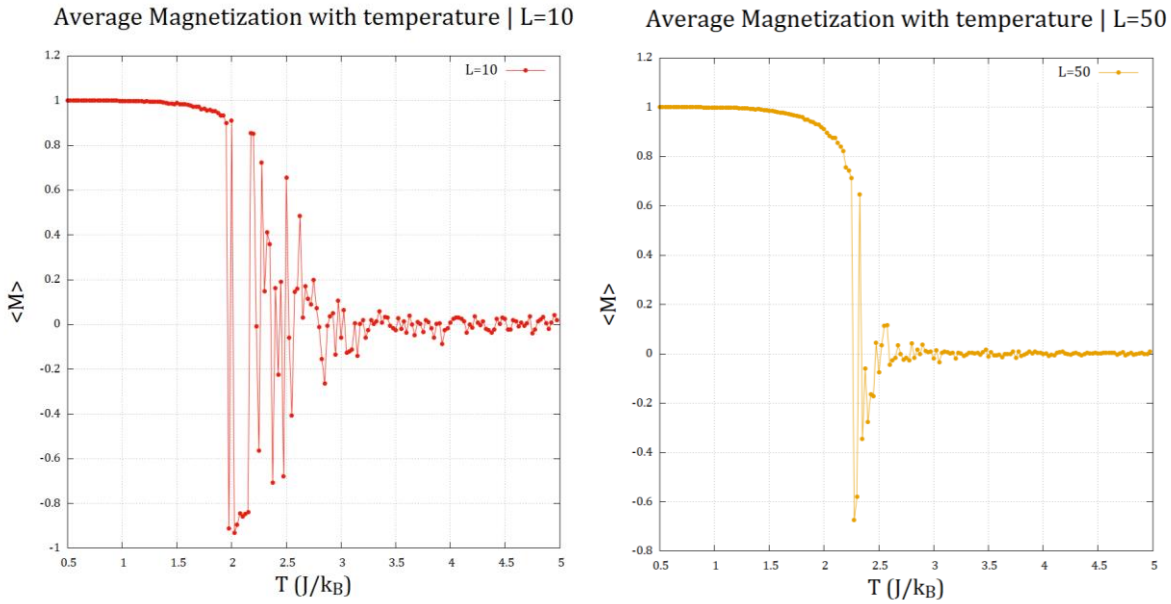

Figure 3.1: Magnetization-Temperature plot for system size $L = 10$ (left) and $L = 50$ (right). Note how $\langle M \rangle$ fluctuates for $2 < T < 3$. For these plots, $dT = 0.025$, total no. of MC steps was 5000, and $\langle M \rangle$ was averaged over the last 100 MC steps.

Looking at the plots above, we notice 2 distinct regions:

- **Ferromagnetic region:** For $T < 2$, we have $\langle M \rangle \approx 1$. This corresponds to all the spins on the grid being aligned up. A non-zero $\langle M \rangle$ in the absence of external field $\boldsymbol{H}$ indicates ferromagnetic behaviour.
- **Paramagnetic region:** For $T > 2.5$, $\langle M \rangle$ approaches 0, indicating that the spins are oriented completely randomly, which indicates paramagnetic behaviour.

For $2 < T < 2.5$, $\langle M \rangle$ fluctuates wildly. Thus, finding the Curie temperature T_C corresponding to transition point using this method is not very reliable.

* Throughout this report, magnetization M has units of k_B

Addressing the fluctuations near T_C

As for why these fluctuations appear near T_C, it is due to a phenomenon in the 2D Ising model called the "**critical slowdown**"[3]. For local update methods such as the metropolis algorithm, this effect is more pronounced.

Increasing system size seems to reduce the fluctuations slightly, allowing us to narrow down T_C between $T = 2.25$ and $T = 2.5$. This is near to the $T_C = 2.27$ value quoted in the assigned textbook [5].

The results in 3D model

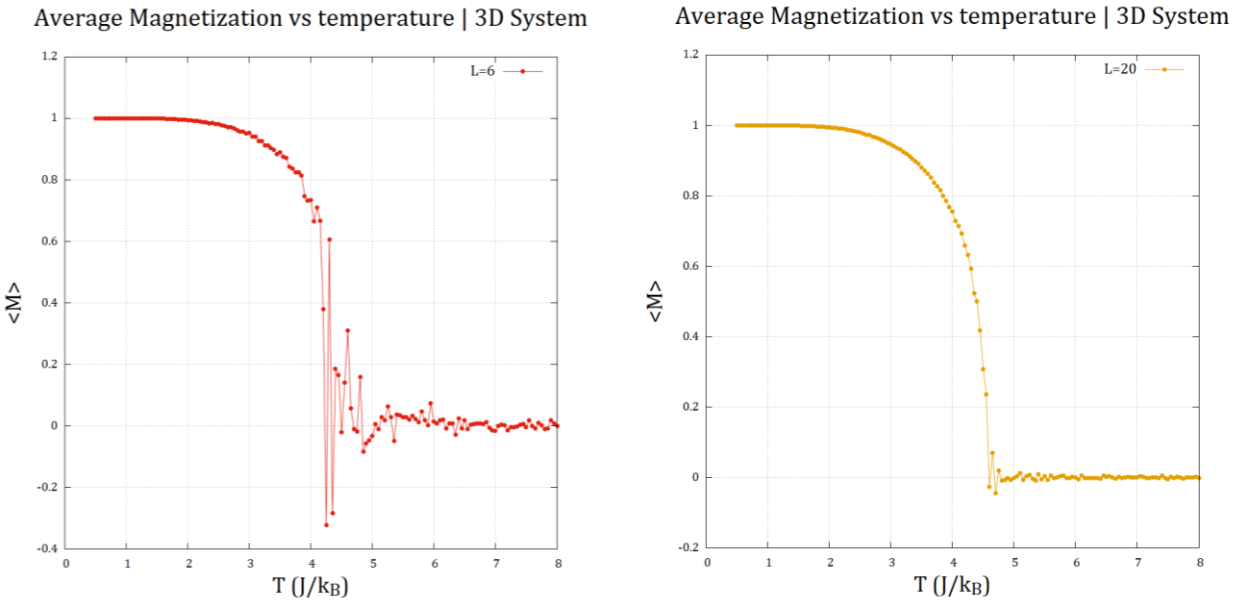

Figure 3.2: $\langle M \rangle - T$ plot for system size $L = 6$ (left) and $L = 20$ (right). Note how $\langle M \rangle$ fluctuates for $4 < T < 5$. For these plots, $dT = 0.05$, total no. of MC steps was 500, and $\langle M \rangle$ was averaged over the last 100 MC steps.

As we can see, the behaviour of the $\langle M \rangle - T$ plot is identical here when we switch to a 3D system. There are clearly 2 distinct regions corresponding to ferromagnetic and paramagnetic behaviour. Even the fluctuations near T_C is replicated.

The only difference here is that the Curie temperature is significantly higher compared to the 2D Ising model. This can be explained by the fact that in 3D, we deal with 6 nearest neighbour interactions instead of 4 in 2D. This would mean that a higher temperature is required to "scramble" the spins.

From the plot for system size 20, we can narrow down T_C between $T = 4.5\, J/k_B$ and $T = 4.8\, J/k_B$

3.2 Variation of susceptibility (χ) & specific heat (C) with temperature

Susceptibility Results

Below we have the plots for susceptibility with varying temperature for 2 system sizes. No external magnetic field H was applied:

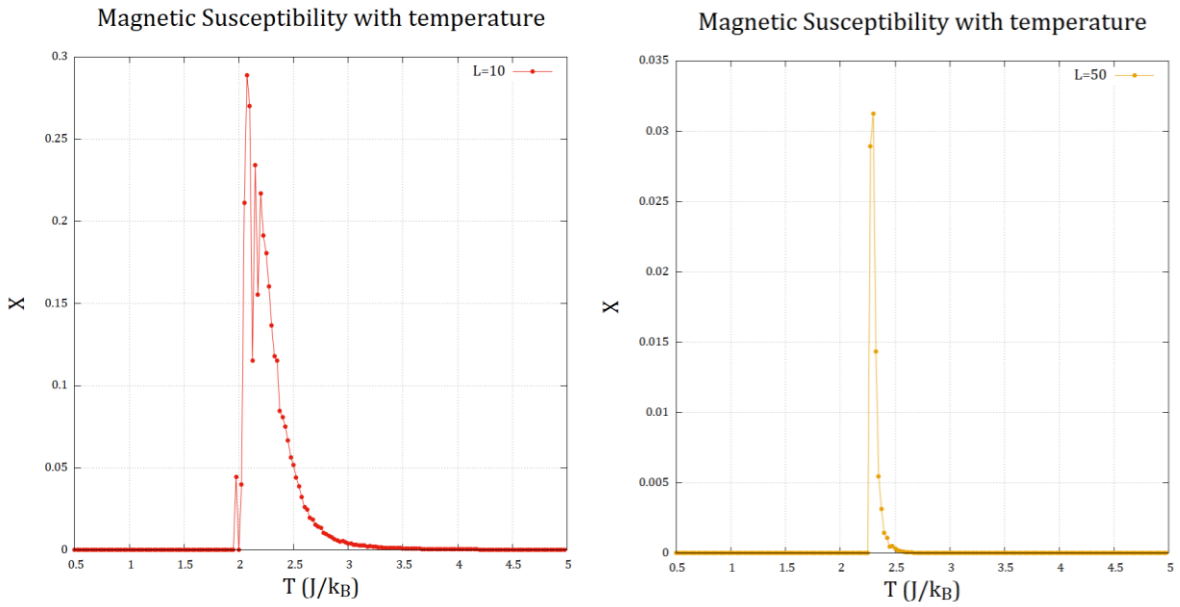

Figure 3.3: $\chi - T$ plots for system size $L = 10$ (left) and $L = 50$ (right). For these plots, $dT = 0.025$, total no. of MC steps was 5000

The fluctuation-dissipation theorem expression for susceptibility that was used for the plots above reads: $\chi = \frac{(\Delta M)^2}{k_B T}$

Where $(\Delta M)^2$ is the variance of magnetization. From the previous section, we know that the magnetization fluctuates around the Curie temperature T_C. This means that the variance will be large near T_C, and will be highest at T_C. From this, we infer that the maximum of the χ in the plots correspond to the Curie temperature. So, this is a much better way to determine T_C compared to $\langle M \rangle$ method.

And as we've said before, below T_C the material is in ferromagnetic state. But in the plots above, the susceptibility below T_C is 0, which is inconsistent with actual ferromagnetic substances which have high χ. This is down to our use of fluctuation dissipation theorem to calculate χ.

From the $\langle M \rangle - T$ plots, $\langle M \rangle \approx 1$ below T_C, with little fluctuation. This means that $(\Delta M)^2 \approx 0$ and thereby $\chi \approx 0$.

The Curie temperature is roughly around $2.08\, J/k_B$ from $L = 10$ plot, and around $2.3\, J/k_B$ from $L = 50$ plot. This is within the range of estimate that we obtained from $\langle M \rangle - T$ plots.

The results in 3D model

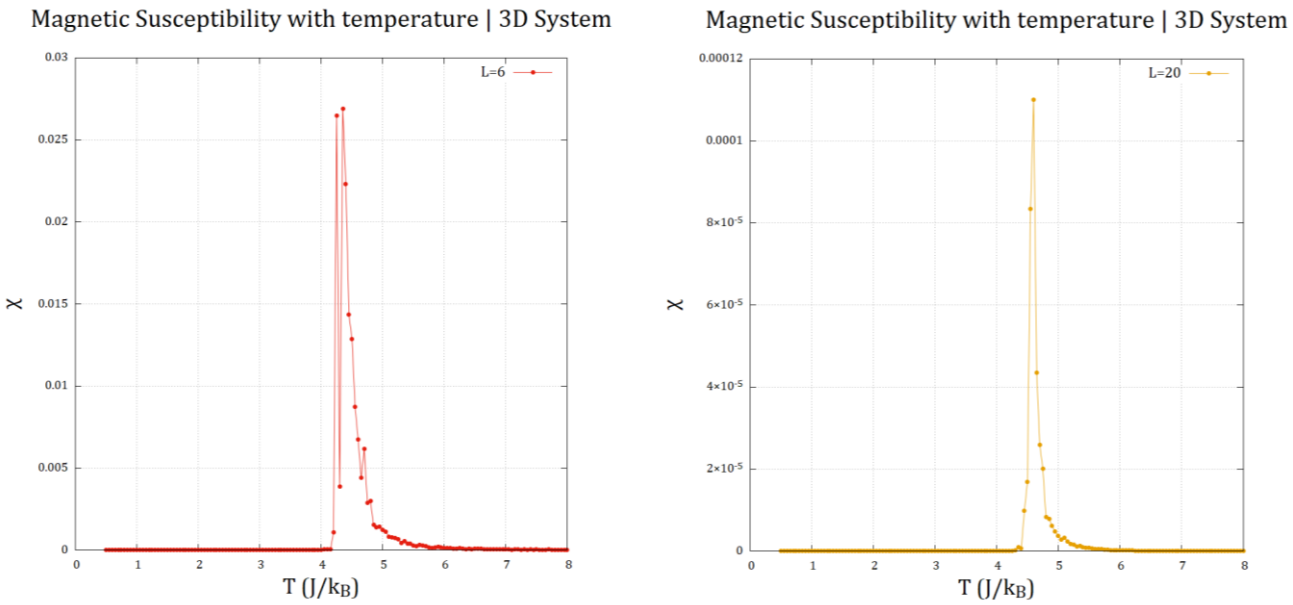

Figure 3.4: $\chi - T$ plot for system size $L = 6$ (left) and $L = 20$ (right). For these plots, $dT = 0.05$, total no. of MC steps was 500.

Here again, the susceptibility behaviour is replicated from the 2D Ising model. The Curie temperature is roughly around 4.46 J/k_B from $L = 6$ plot, and around 4.6 J/k_B from $L = 20$ plot. These are within the range of estimate obtained from $\langle M \rangle - T$ plots.

Specific Heat Results*

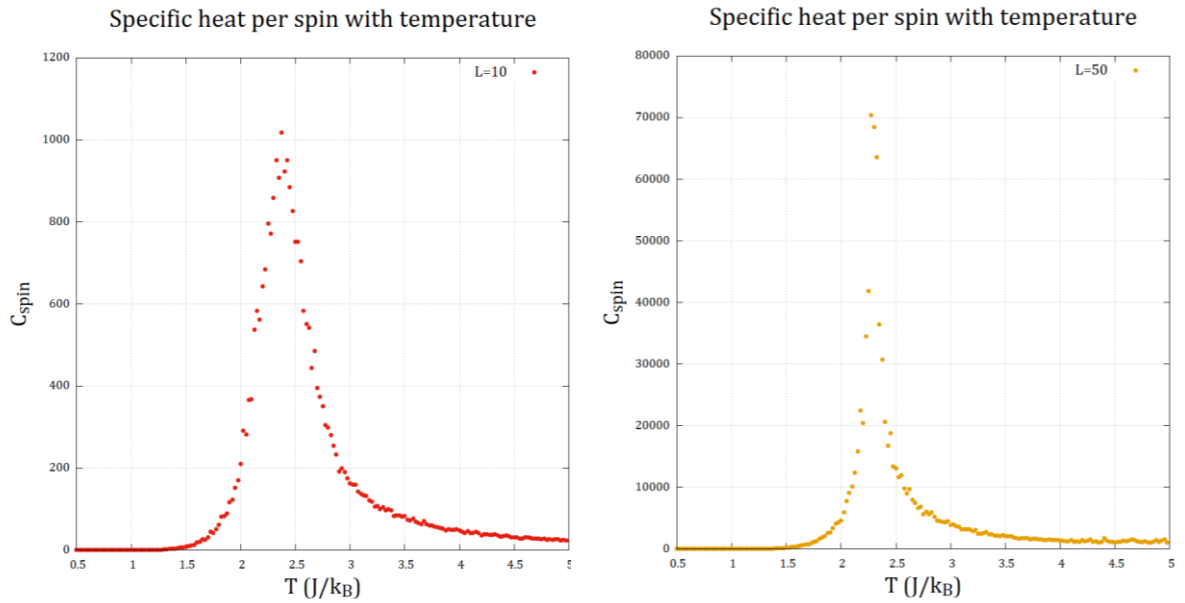

Figure 3.5: $C_{spin} - T$ plots for system size $L = 10$ (left) and $L = 50$ (right). For these plots, $dT = 0.025$, total no. of MC steps was 5000. The magnetic field B was set to 0.

* **Specific heat & C_{spin} throughout this report are expressed in units of k_B**

The fluctuation-dissipation theorem for specific heat tells us: $C = \frac{(\Delta E)^2}{k_B T^2}$

For similar reasons to why the maxima of χ was at T_C, we can also convince ourselves that the variance of energy $(\Delta E)^2$ is maximum near T_C.

In figure 3.5, we don't actually plot specific heat, but its value per individual spin in the grid, i.e. $C_{spin} = C/L^2$. We can clearly see that the peak is roughly at 2.375 J/k_B from $L = 10$ plot, and at 2.273 J/k_B from $L = 50$ plot. This is within the range of estimate that we obtained from $\langle M \rangle - T$ plots.

The results of 3D model

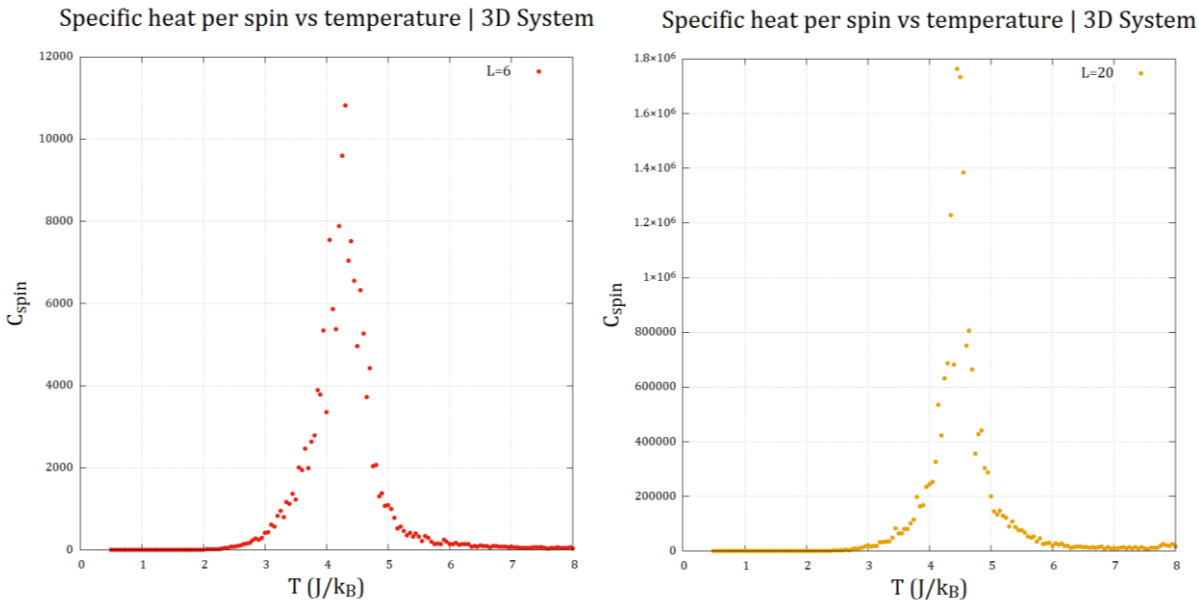

Figure 3.6: $C_{spin} - T$ plots for system size $L = 6$ (left) and $L = 20$ (right). For these plots, $dT = 0.05$, total no. of MC steps was 500. The magnetic field B was set to 0.

By now, it shouldn't be surprising that the behaviour for specific heat per spin for 3D is not different than that in the 2D Ising model. And here again, the peaks of C_{spin} at 4.23 J/k_B from $L = 6$ plot, and at 4.45 J/k_B from $L = 20$ plot indicate that the phase transition is characterized by the maxima in specific heat.

With this, we have now seen 3 possible ways to identify the Curie temperature.

3.3 Existence of hysteresis

One of the identifiable characteristics of a ferromagnetic material is the existence of hysteresis. Specifically, this implies that the curve of magnetization with the magnetic field forms a closed curve with an enclosed area. The bigger the area, the harder it is to demagnetize a ferromagnet.

We observe hysteresis loops both in 2D & 3D. Below we show the $M - B$ curves for various temperatures*:

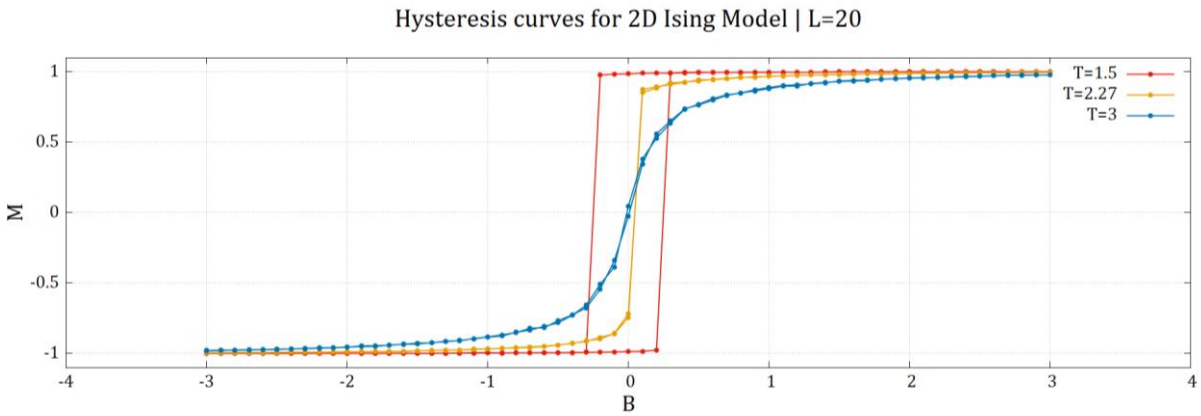

Figure 3.7: $M - B$ curves obtained for the 2D Ising model for $T < T_C$ (red), $T \approx T_C$ (yellow) and $T > T_C$ (blue). For this plot, we used $L = 20$, $dB = 0.1$ maximum MC steps to be 5000, with $\langle M \rangle$ averaged over the last 100 MC steps.

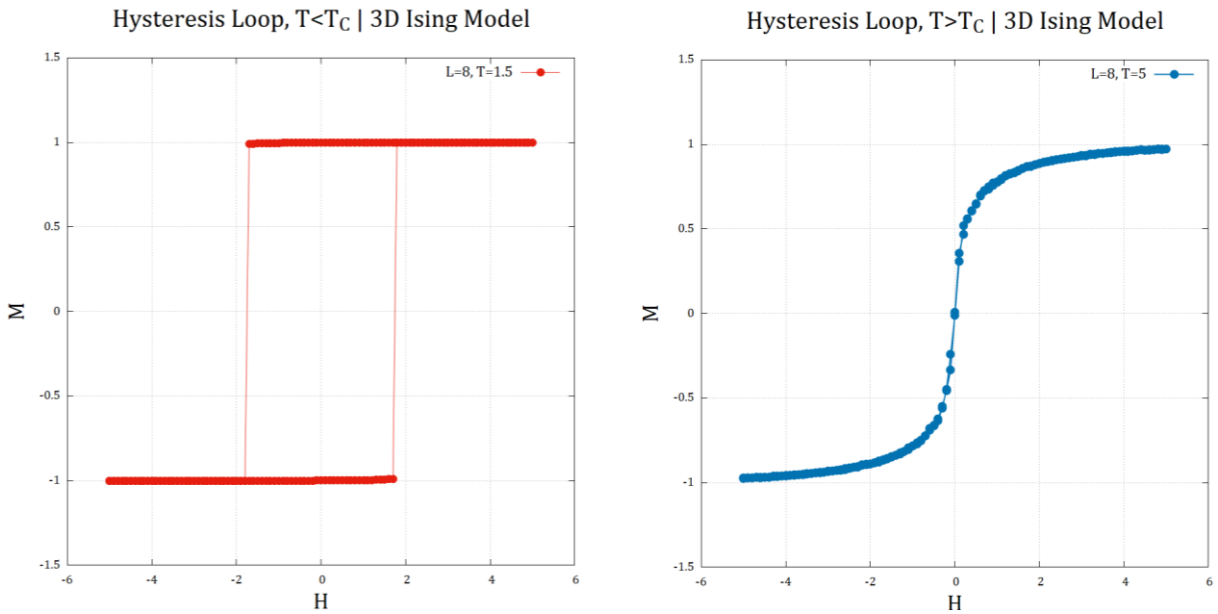

Figure 3.8: $M - B$ curves obtained for the 3D Ising model for $T < T_C$ (red) and $T > T_C$ (blue). For this plot, we used $L = 8$, $dB = 0.1$, maximum MC steps to be 500, with $\langle M \rangle$ averaged over the last 100 MC steps. **NOTE:** H here is a typo. The X axis is meant to represent magnetic field B. Also, for $T > T_C$, the curve is not a loop (that was a blunder)

* Temperatures are all in J/k_B units

3.4 Effect of system size

One thing that we have overlooked so far in our results is the effect of increasing system size on the properties. Below we summarize how system size effects each of the properties discussed so far:

Effect on $\langle M \rangle - T$ curve

In our results, we have already hinted the effect of system size on $\langle M \rangle - T$ curve. If we look back at figure 3.1, we can indeed notice that the fluctuations near T_C reduces significantly as we increase system size. This is true for both 2D & 3D Ising model. This will be key in understanding the effects of system size on other properties.

Effect on $\chi - T$ curve

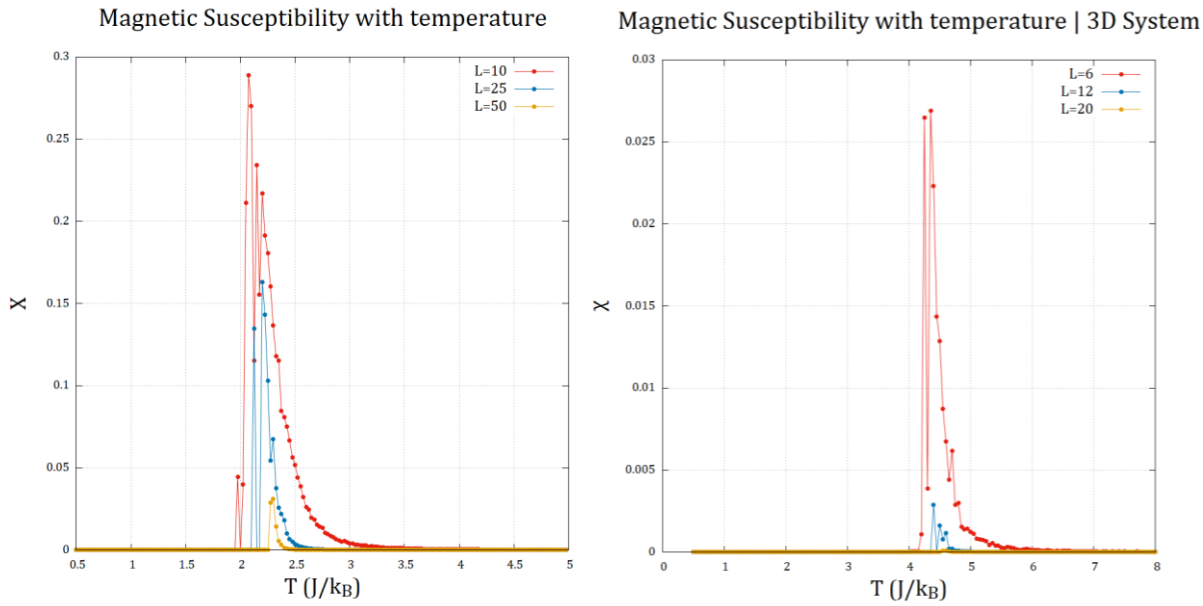

Figure 3.9: $\chi - T$ curves for various system sizes (L) for the 2D (left) & 3D (right) Ising model. The parameters of the simulation are unchanged from those in section 3.2

We observe the following trends from the above curve:

- The value of χ decreases as we increase the system size for both 2D & 3D. The rate of decrease is more significant for 3D system.
- The Curie temperature T_C increases, as the peak of $\chi - T$ curve shifts to the right.

The reason behind these observations comes from the expression we used to calculate χ, which was from fluctuation-dissipation theorem: $\chi = \frac{(\Delta M)^2}{k_B T}$

We know that increasing system size causes a reduction in $(\Delta M)^2$. This effect is more pronounced for the 3D system (compare the fluctuations in figures 3.1 & 3.2). This corresponds to a reduction in the peak of $\chi - T$ curve. But the reason for higher T_C is unclear. This needs to be looked into further.

Effect on $C_{spin} - T$ curve

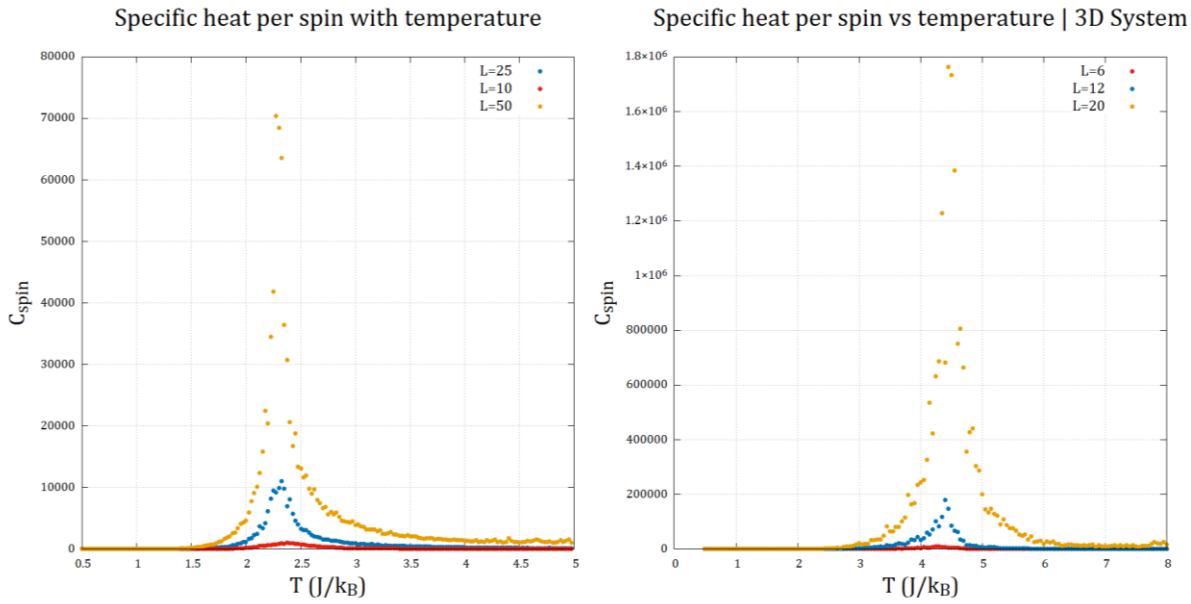

Figure 3.9: $\chi - T$ curves for various system sizes (L) for the 2D (left) & 3D (right) Ising model. The parameters of the simulation are unchanged from those in section 3.2

We can deduce the following from the plots above:

- The value of C_{spin} increases as we increase the system size for both 2D & 3D. The rate of increase is more significant for 3D system.
- The Curie temperature T_C decreases, as the peak of $C_{spin} - T$ curve shifts to the right ever so slightly.

The reason behind these observations comes from the expression we used to calculate C_{spin}, which was from fluctuation-dissipation theorem: $C = \frac{(\Delta E)^2}{k_B T^2}$

We know that increasing system size causes an increase in $(\Delta E)^2$ (as E is an extrinsic property) due to the increase in number of spins in the grid. In 2D, the increase with L is L^2, whereas it's L^3 for the 3D system*.

For the Curie Temperature, we see that in 2D, the peak of C_{spin} shifts to the left (i.e. T_C decreases). The opposite is true in 3D. Although the increase in C_{spin} is nominal. This is quite an interesting development that needs further investigation.

* We're not claiming that ΔE scales as L^{dim}, just that ΔE is expected to increase with system size

3.5 Runtime analysis

One of the factors that limits the usefulness of a simulation method is its runtime. If the **algorithmic complexity** of the method employed scales horribly (refer to figure 3.10) with input size, it would be wise to look for better methods that are more efficient.

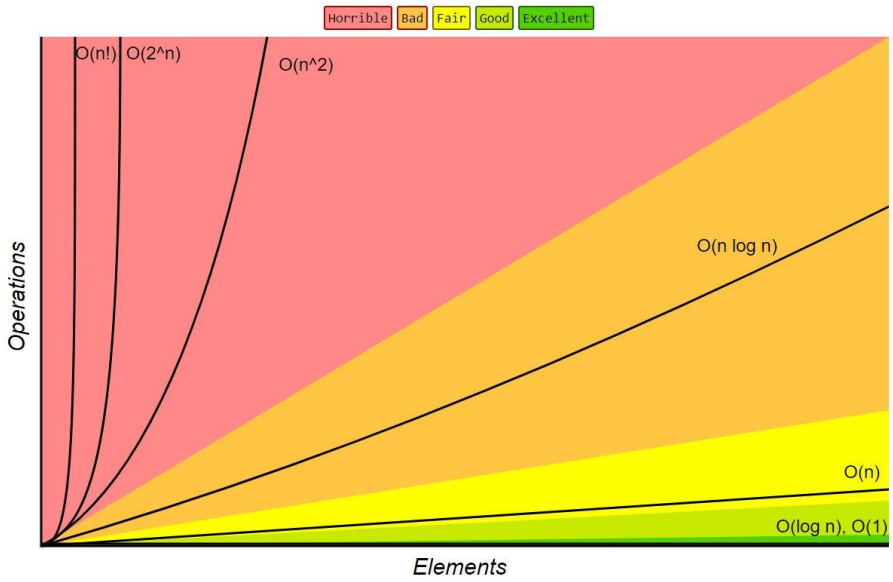

Figure 3.10: Order of growth of algorithms specified in Big-O notation. [Source: Big-O Cheat Sheet, 2016]

Below we present our results for runtime measurements for increasing system size, for which we used the built in `cpu_time()` function in Fortran 90. This gives us the *processor time** taken up by the program from start to finish.

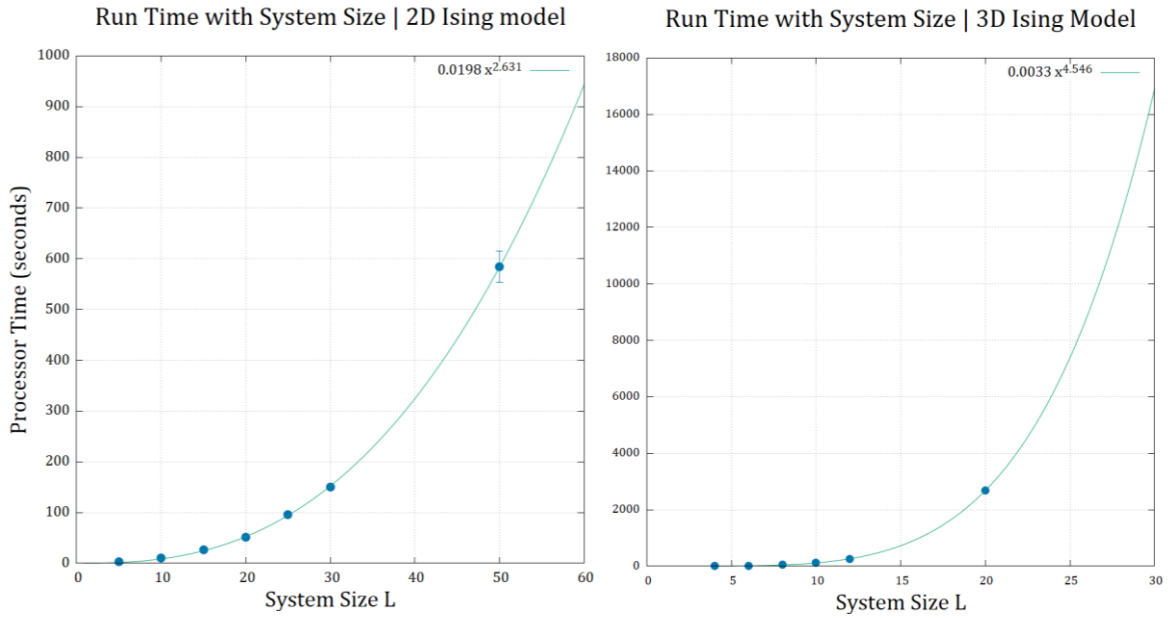

Figure 3.11: Processor time with best fit curves for 2D (left) & 3D (right) Ising models

* Which we found was close the measured time.

The runtimes were measured for the same parameters, only varying system size (the edge length L). We found that a polynomial function of the form. The best fit lines for runtime $\tau(L)$ were as follows:

- For 2D: $\tau(L) = 0.0198\ L^{2.631}$
- For 3D: $\tau(L) = 0.0033\ L^{4.546}$

According to figure 3.10, the Monte Carlo Metropolis algorithm is classified as horrible algorithm [6]. So, using a better algorithm such as Wolff algorithm [4] is something that we must consider for future work.

But the fit is not what we expected. While we did expect the algorithm to run in polynomial time, we expected L to scale with the dimension of the Ising model, i.e. $\mathcal{O}(L^2)$ for 2D & $\mathcal{O}(L^3)$ for 3D, as the Monte Carlo sweep over the grid is repeated the most times in the code, and time needed to execute those parts are proportional to L^{dim}. But regardless, the Metropolis algorithm is not what one would use to simulate a very large system with Ising model.

4 Effect of exchange energy J on system properties

4.1 Variation of system properties with J

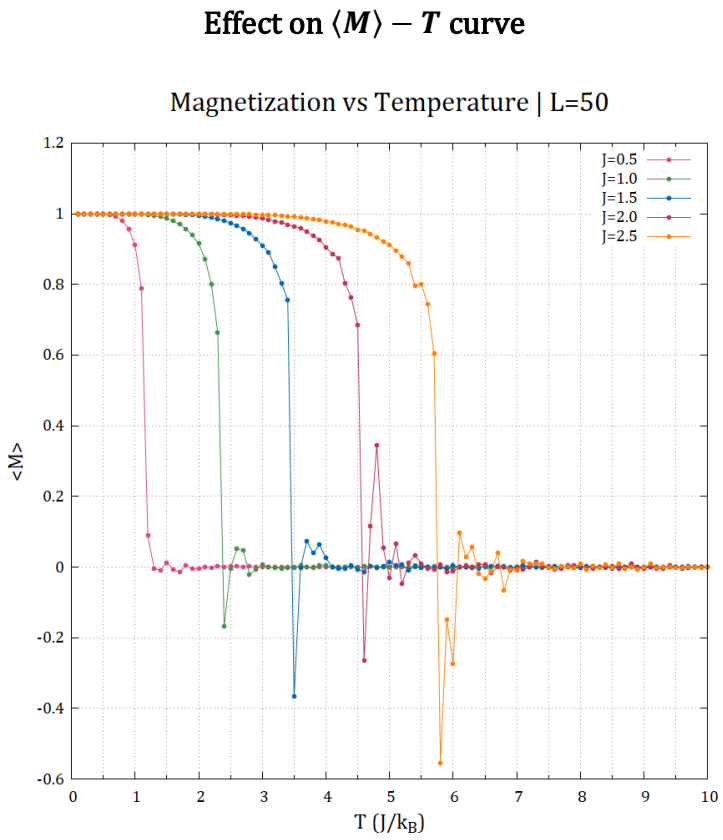

Figure 4.1: $\langle M \rangle - T$ plots for increasing exchange energy strengths

As shown in figure 4.1, increasing the exchange energy constant increases the value of the Curie temperature T_C. T_C indicates to what extent a ferromagnet can withstand increase in temperature before turning into a paramagnet. If we look closely at figure 4.1, it seems that T_C changes almost linearly with J.

Effect on $C - T$ curve*

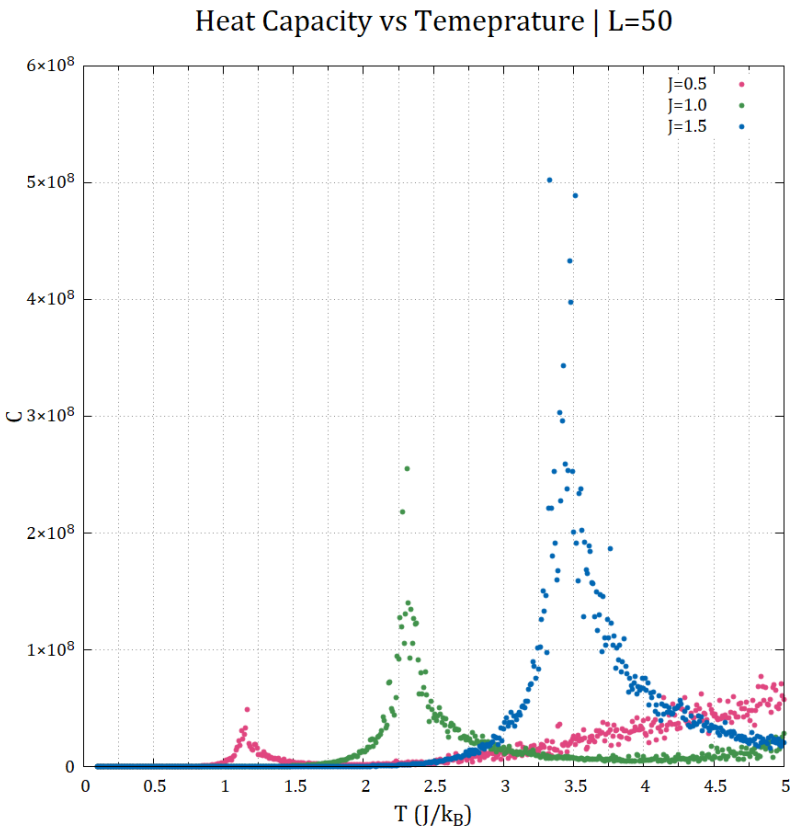

Figure 4.2: $C - T$ plots for increasing exchange energy strengths

The same behaviour mentioned above is replicated here. As we increase the coupling constant the Curie temperature increases. Again, we observe the linear trend. The specific heat capacity also increases as we increase J. This makes sense, as increasing exchange energy would make it more difficult to "scramble" the spins in the grid.

Effect on $\chi - T$ curve

Here again, we observe a direct linear relationship between J and Curie temperature (which is indicated by the maxima of $\chi - T$ curve). The magnitude of susceptibility decreases as we increase J. But the decrease here is not linear, as we would expect by now. Instead, the χ value appears to plateau as we increase the strength of J (as seen in figure 4.3). This indicates that the variance of magnetization $(\Delta M)^2$ itself is effected by J. This needs further investigation.

* We plotted the heat capacity here, and not the heat capacity per spin

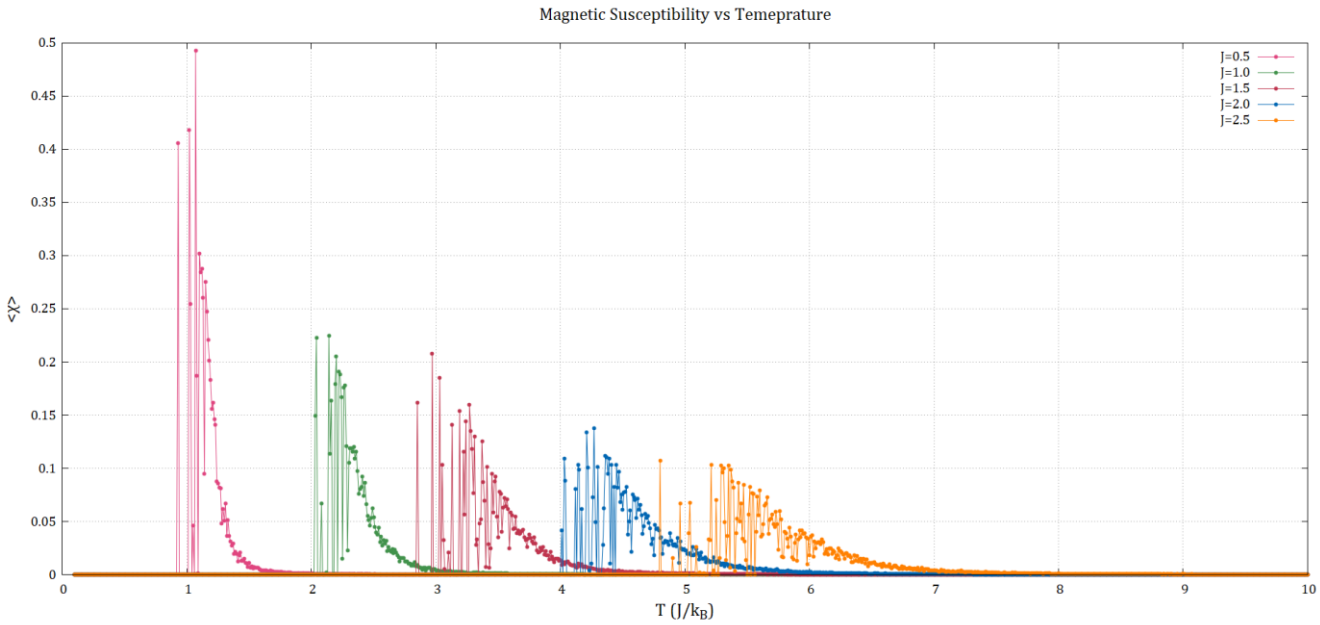

Figure 4.3: $\chi - T$ plots for increasing exchange energy strengths. Here the system size was $L = 10$

4.2 Effect on Hysteresis

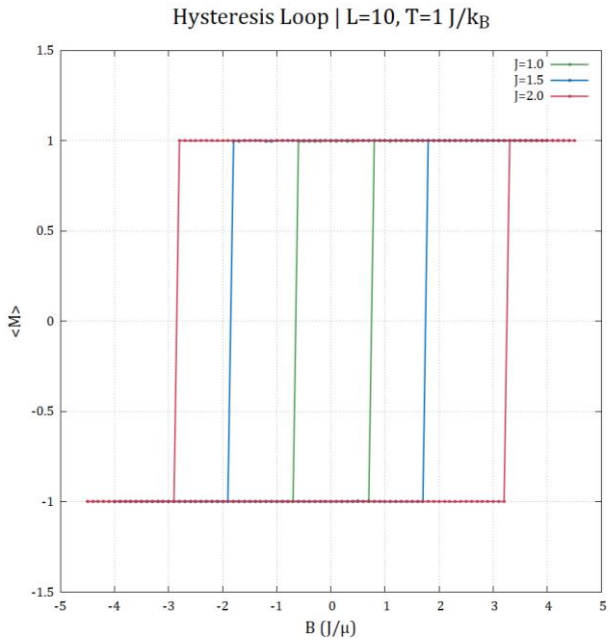

Figure 4.4: Hysteresis loops for increasing strengths of J

The area of hysteresis loop indicates how much energy the system needs to be demagnetized [2]. In figure 4.4, at a fixed temperature*, as we increase the coupling constant as the hysteresis loop area increases. This shows that the material becomes a stronger ferromagnet due to increasing J. This means that it needs more energy to be demagnetized.

* The temperature itself is in units of J, we didn't take that into account.

4.3 Effect on Coercive Field (B_C)

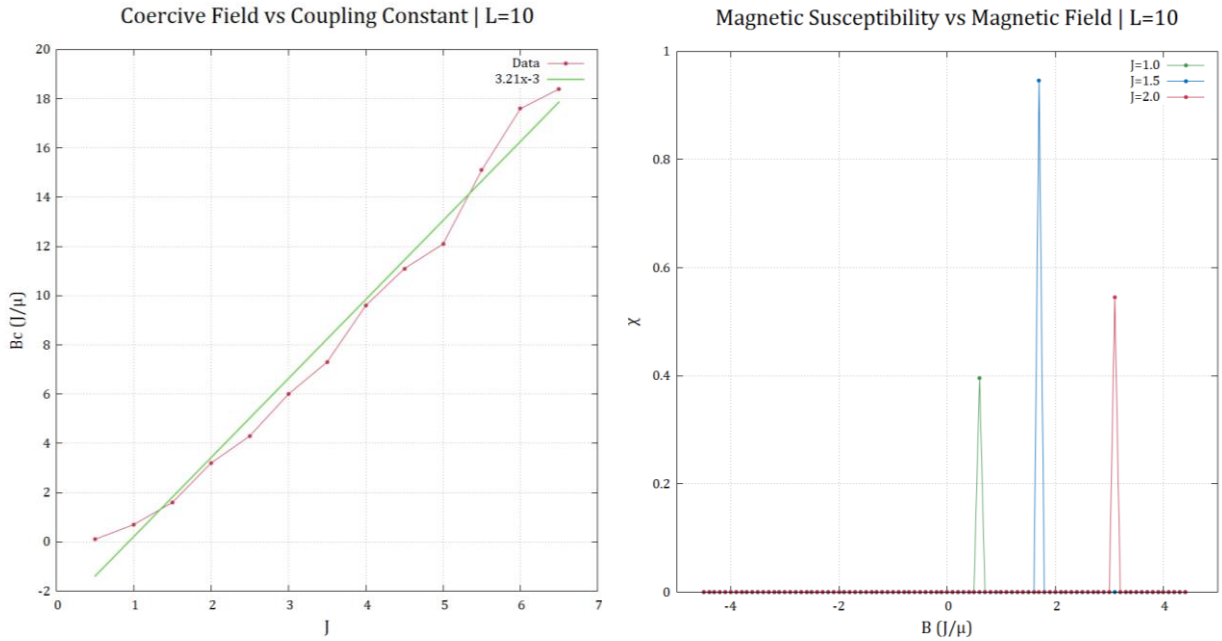

Figure 4.5: The best fit line of coercive field B_C with J (left) and $\chi - B$ plot (right)

Coercive field B_C is the value of magnetic field for which the magnetization of a ferromagnet is reduced to 0. The non-zero value of susceptibility in figure 4.5 indicates the coercive field B_C*. Also, coercive field's value can be known from the hysteresis loop when the magnetization state of the system changes.

By fitting the $B_C - J$ plot, we obtain a linear relationship. The slope is found to be 3.21. You can see in the figure that the coercive field for J=0.5 is 0, which means the system is in paramagnetic phase! This would be discussed later and the effect of the fixed temperature on studying the effect of J.

Note: Since we took $J = 1$ in formulating the Ising model, units of T will be changed if we change J. So, our investigation about the relation between coupling strength and coercive field must consider this into account. Because T is not consistent throughout, T_C was different for each run. That is what led to zero coercive field for $J = 0.5$ which meant that the system became paramagnetic phase.

For future work, it should be considered to change the temperature for each value of J and keep it the Curie temperature consistent at all values of J.

* Here, χ was obtained from the fluctuation-dissipation theorem result

5 Simulating antiferromagnetism with Ising model

Simulating antiferromagnetism using the Ising model is quite straightforward. We just need to change the sign of J, which would favour neighbouring spins to anti align with each other. Also, the spins on the grid were made to alternate between ± 1 spins.

5.1 Existence of an antiferro-para phase transition

As in a ferromagnetic material, there is also a phase transition in antiferromagnetic material due to changing temperature. As the temperature rises, thermal fluctuations increase and destroy the order of spins making them randomly aligned. In other words, the material is now paramagnetic.

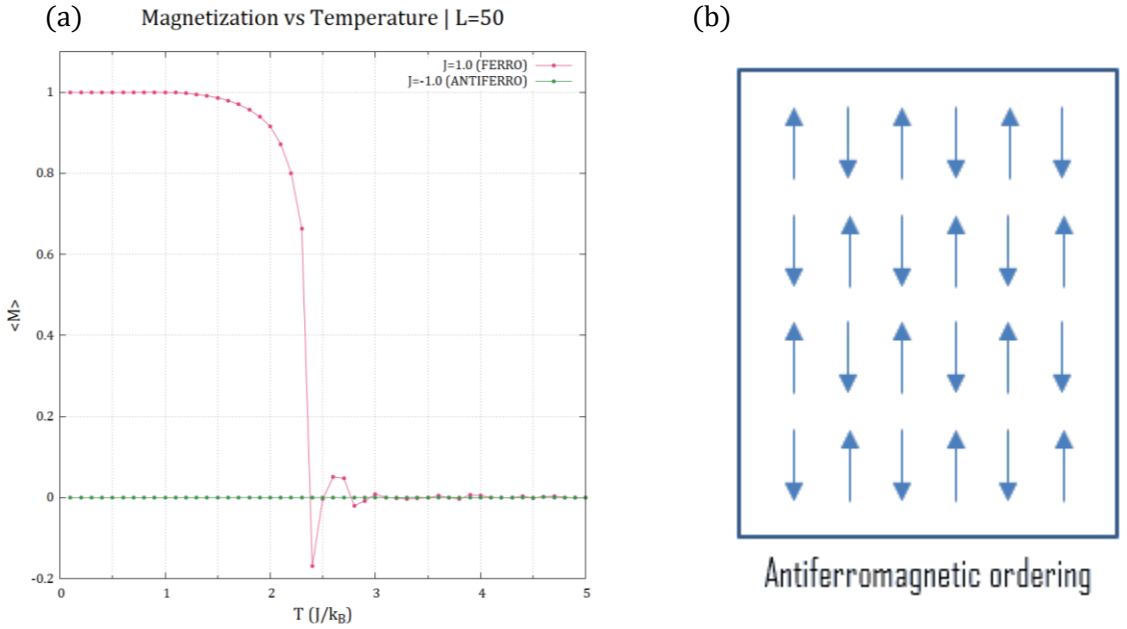

Figure 5.1: (a) $\langle M \rangle - T$ plot of ferro and antiferro systems
(b) Antiferromagnetic ordering [Source: materialproperties.org]

To investigate this phase transition, we plotted the average magnetization with the temperature, as we would usually do for a ferromagnetic material. A comparison between ferro- and antiferro- material phase transition is shown in figure 5.1(a).

There is no visible phase transition in $\langle M \rangle$ for an antiferromagnetic material. That's because the spins in antiferro-material align antiparallel to each other (figure 5.1(b)) so $\langle M \rangle$ is zero. Also, for paramagnetic material, due to randomness of the spins' directions makes the magnetization zero.

For that reason, the phase transition cannot be seen by studying magnetization with the temperature for antiferromagnetic material. Another property will be studied to capture the phase transition.

5.2 Estimating the Néel temperature

Néel temperature T_N is equivalent to the Curie temperature for antiferromagnetic materials. At this temperature, ordered arrangement of spins disappears entirely and the material becomes paramagnetic. To estimate Néel temperature we studied the susceptibility with the temperature. We used the Curie-Weiss law [2], which gives us:

$$\chi = \frac{C}{T + T_N}$$

Where C is some constant. By plotting the reciprocal of susceptibility $1/\chi$ with temperature T, the intersection of the fitting line with the x-axis gives us the Néel temperature.

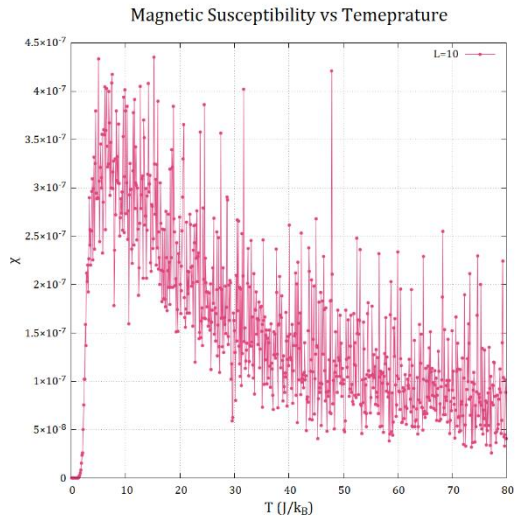

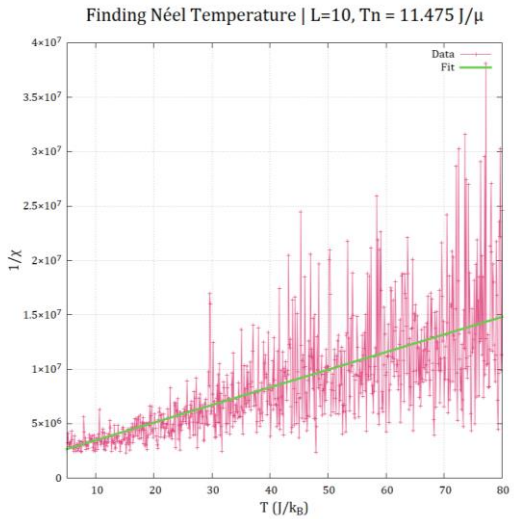

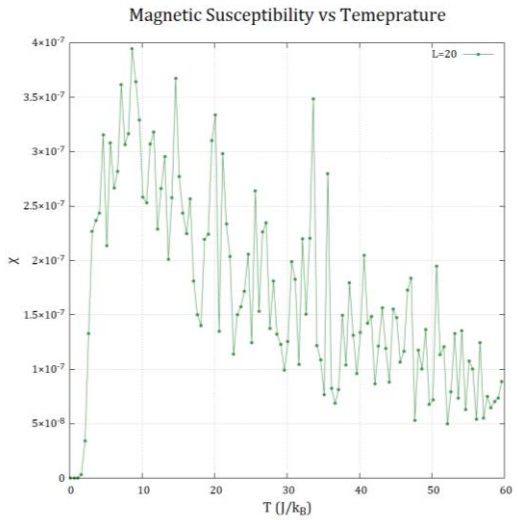

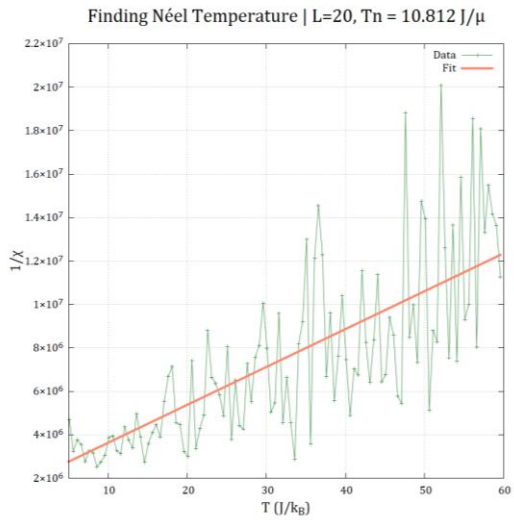

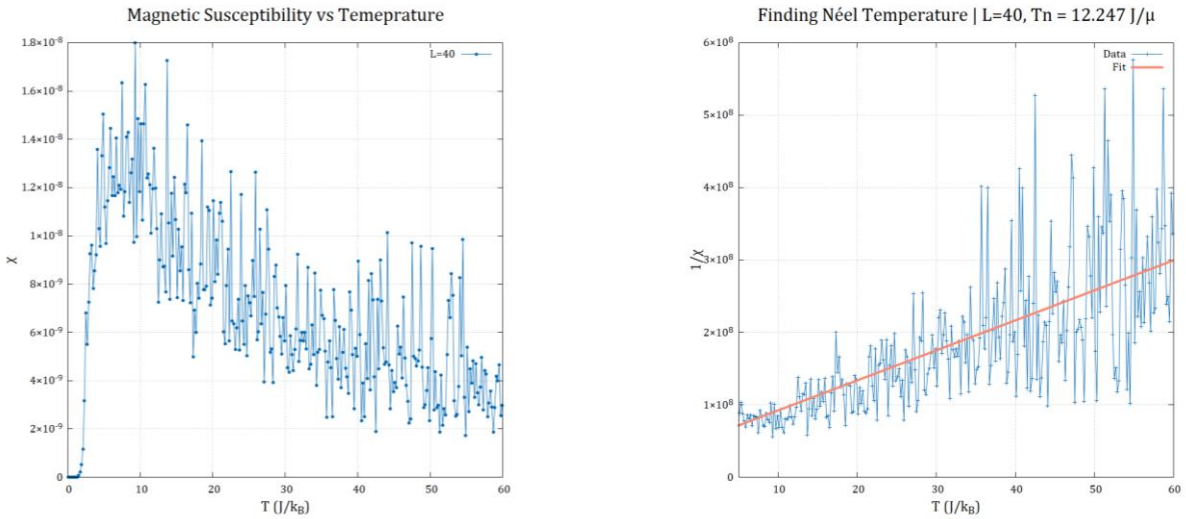

Figure 5.2: Finding the Néel temperature T_N by applying Curie-Weiss law for various system sizes. T_N is obtained by fitting $1/\chi - T$ curve with the best fit line.

In figure 5.2, the plot for $\chi - T$ for system size $L = 10$ units is too noisy in the paramagnetic phase. So, we tried to increase the system size and increase the temperature step (dT) in the code to get less noisy plots. Since we didn't have time to average over multiple runs, we went ahead and fit the formula anyway.

From the plots of $1/\chi - T$ for the 3 graphs in figure 5.2, we got the Néel temperature T_N as 11.475, 10.812 and 12.247 (in J/k_B) for system sizes 10, 20 & 40 units respectively. These aren't too far off each other. So, even if these results are wrong, they are somewhat consistent. We should however add a caveat that Curie-Weiss law is derived from mean field theory, which may not applicable to the Ising model.

6 Considering general spin direction

One of the simplifications made in the classic Ising model is that the spins can only point either up or down. To study a more realistic system, we allow the spins to have any possible orientation while still remaining on the 2D grid. The spins still have unit magnitude

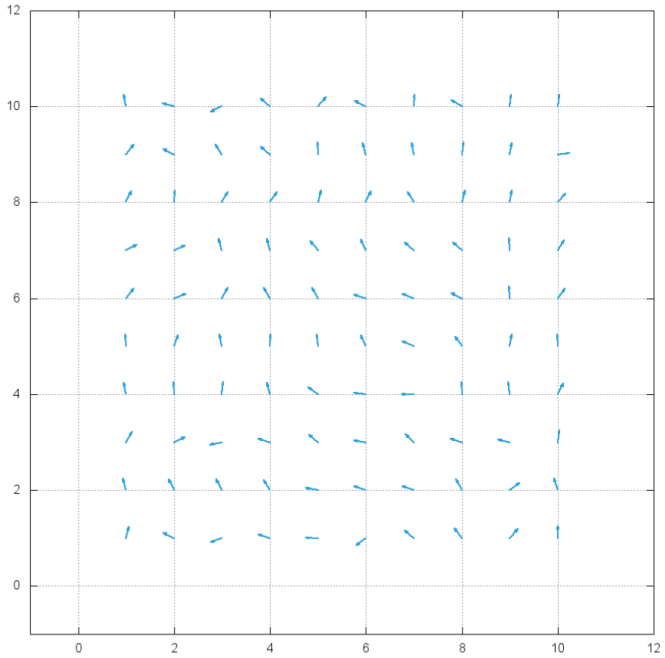

Figure 6.1: Implementation of general spin direction to the 2D Ising model on a 10×10 grid

The required modifications that need to be made to the regular Ising model are listed below:

- The spin interaction term is now: $J(\boldsymbol{S_i} \cdot \boldsymbol{S_j}) = J \times \cos(\theta_{ij})$
  Where $\theta_{ij} = \theta_i - \theta_j$
- The magnetic interaction term becomes: $-\boldsymbol{S_i} \cdot \boldsymbol{B} = -B \sin\theta_i$
  This assumes that $\boldsymbol{B}$ points along $\theta = \pi/2$.
- We no longer "flip" the spins. Instead, we introduce a random orientation between 0 and 2π.

6.1 Existence of ferro-para phase transition

We were able to demonstrate the existence of a ferro-para transition by animating the spin states with rising temperature in the absence of B field. For each temperature, the last snapshot of the spin grid was taken. In the animation, there is clearly a distinct change in behaviour from largely aligned spins ($\theta \approx 0$) to completely random alignment.

Shown below are some snapshots for the animation starting from $T = 0.5$ to $T = 3.95$ (in J/k_B units):

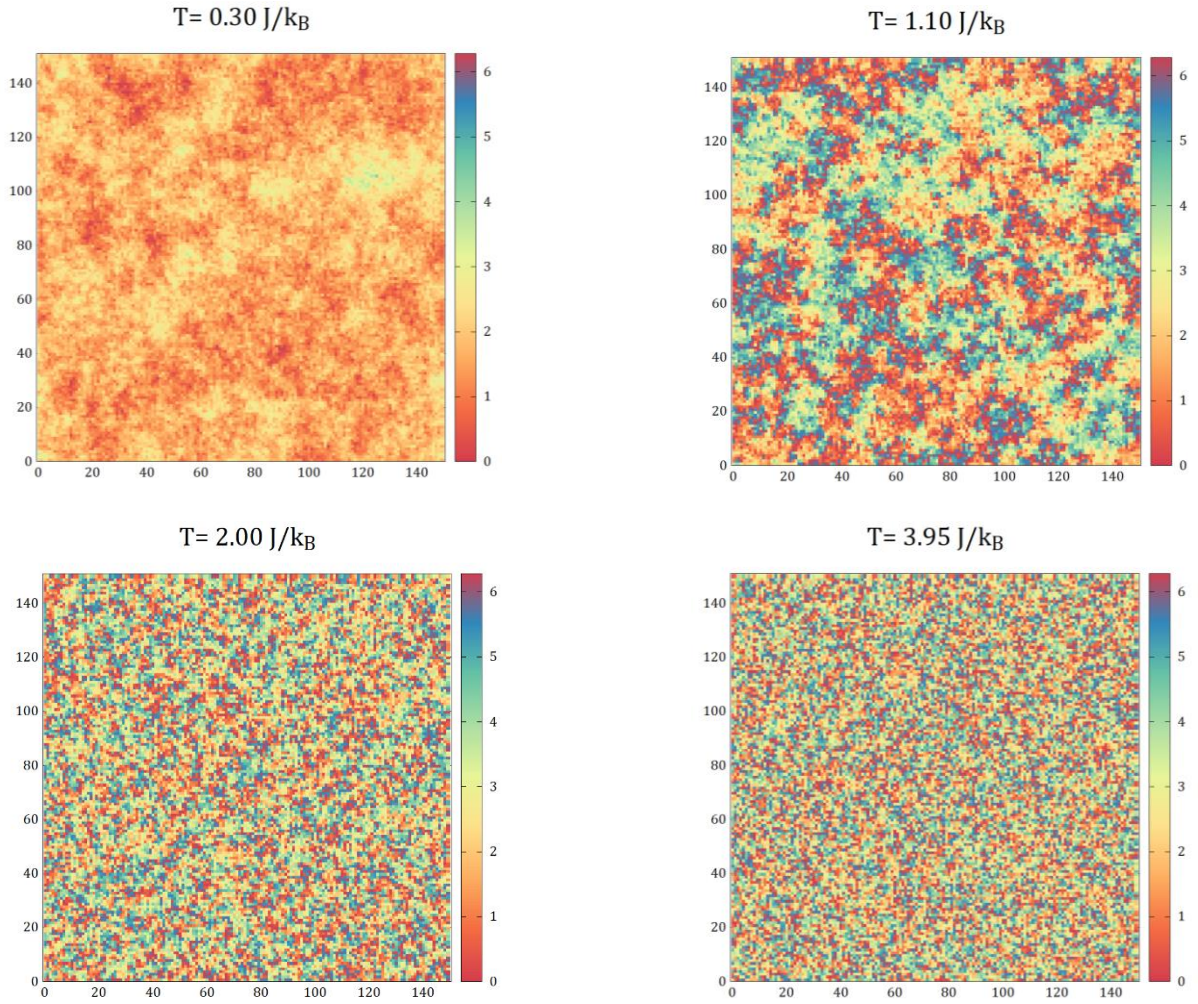

Figure 6.2: Demonstration of ferro-para transition for Ising model with general spin directions. For these plots, the system size was 150, $dT = 0.05$, maximum MC steps was 1000. The colour legend represents $0 < \theta < 2\pi$.

At the beginning of each MC step, the spins are assigned randomly. Although this is a qualitative argument, it does have some merit. At $T = 0.3$, we see that the spins are *nearly* aligned with the magnetic field, indicating a net positive $\langle M \rangle$. This confirms the existence of a distinct ferromagnetic phase, albeit weaker than that of the classic 2D Ising model (qualitatively speaking).

As T increases, we see some clusters emerging, all of which are aligned in the same direction (See $T = 1.1$). As we approach $T = 3.95$, the spins are completely randomly aligned. This corresponds to $\langle M \rangle \approx 0$, indicating a paramagnetic behaviour.

At this point, we can convince ourselves of a phase transition and a corresponding Curie Temperature T_C. We speculate that this will be lower than in standard 2D model, as in a general spin system, there are more opportunities to induce fluctuations (as a larger range of θ is available for "flips").

6.2 Existence of Hysteresis

To test whether a hysteresis loop exists, we chose a low temperature that is likely less than T_C ($T = 0.5$) and varied the magnetic field from $B = -5$ to $B = 5$ (in J/μ) units. Snippets from the resulting animation of spins are shown below:

- Below, we see the system near saturation magnetizations:

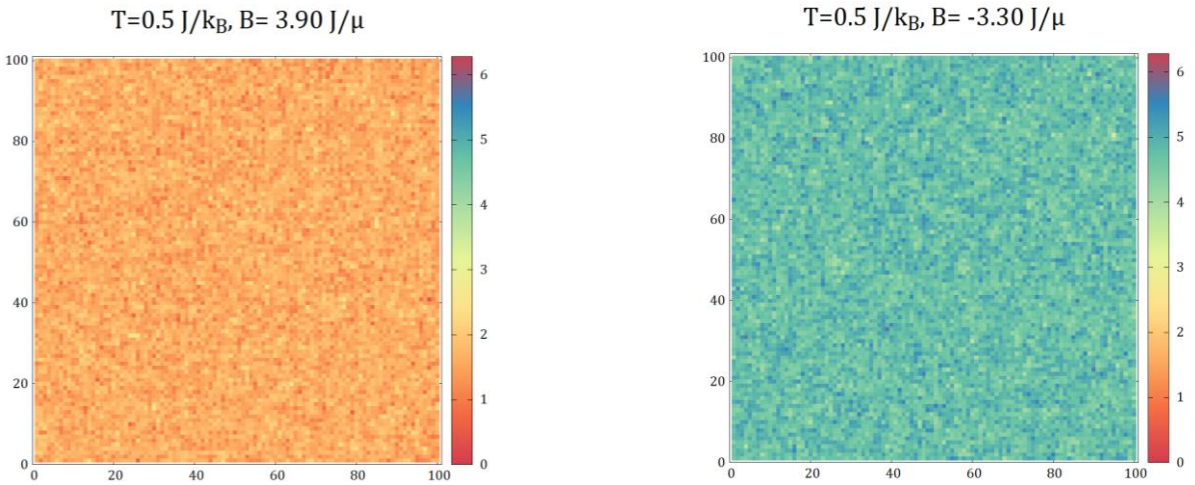

In these states, most spins are aligned along $\theta \approx \pi/2$ or $\theta \approx 3\pi/2$, i.e. nearly aligned with the direction of B field.

- These plots show the system when the field is nearly equal to the coercive field B_C. These correspond to the B fields for which the direction of majority of the spins switch directions. T
- The values of coercive fields are low compared to the regular 2D model with similar parameters. This suggests that the ferromagnet formed by general spin model is softer than the regular 2D counterpart.

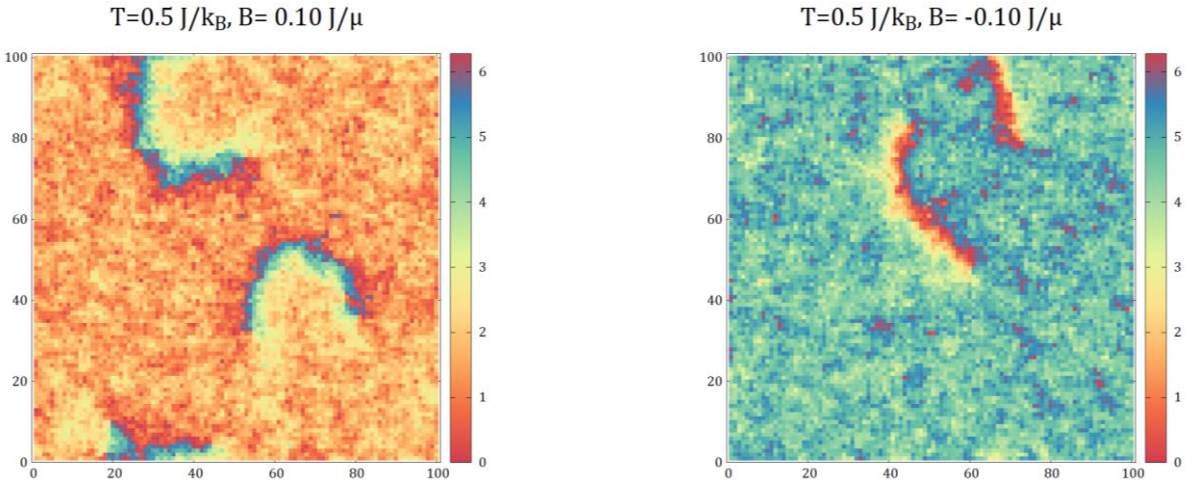

7 Conclusion

Over the course of this project, we studied magnetism using the Ising model and investigated the effect of system size, exchange energy strength on specific heat, susceptibility and magnetization. We demonstrated the existence of hysteresis and studied the effect of exchange energy on it. We've also extended the classic Ising model from 2D to 3D and found that the critical temperature almost doubled.

We then simulated antiferromagnetism and identified the Néel temperature corresponding to phase transition. We've introduced general spin direction to the Ising model and studied the possible phase transition and hysteresis qualitatively.

We also quantified the runtime of Monte Carlo Metropolis algorithm, and found it to perform poorly with large system sizes. We would like to simulate Ising model with non-local update methods that are more efficient. Also, we would like to implement further nearest neighbour interactions and see the effect on properties. Another goal would be to obtain the critical exponents [7] of the Ising model both in 2D & 3D.

The Ising model is a simple yet powerful simulation tool that is able to capture complicated phenomenon such as magnetism. We really enjoyed working on it.

References

[1] Universality class - Wikipedia. En.wikipedia.org. (2022). Retrieved 10 June 2022, from https://en.wikipedia.org/wiki/Universality_class.

[2] Chikazumi, S., Chikazumi, S., & Graham, C. D. (1997). Physics of Ferromagnetism. Amsterdam University Press

[3] Walter, J. C., & Barkema, G. (2015). An introduction to Monte Carlo methods. Physica A: Statistical Mechanics and Its Applications, 418, 78–87. https://doi.org/10.1016/j.physa.2014.06.014

[4] Viot, Pascal. (2011). Numerical Simulation in Statistical Physics common lecture in Master 2 “Theoretical physics of complex systems” and “Modeling, Statistics and Algorithms for out-of-equilibrium systems.

[5] Giordano, N. J., & Nakanishi, H. (2006). Computational Physics. Prentice Hall.

[6] Dineshpathak, A. (2022, February 19). Algorithmic Complexity. Devopedia. https://devopedia.org/algorithmic-complexity

[7] Jäderlund, T. (2020). A scaling approach to critical exponent calculations for the 2D Ising model.